DOI: 10.7860/JCDR/2026/85021.24209

Original Article

Others Section

A Convolutional Neural Network (CNN)-based Approach for Lung Cancer Detection Leveraging Classical Edge Detection Techniques: An AI-based Retrospective Study

SAURAV MALI[1], ANKUR MUKHERJEE[2], BIREN P PARIKH[3], SANJIBAN PATRA[4], SAMRAT BORDOLOI[5], SANCHAITA RAJKHOWA[6], SUBRATA SINHA[7]

ABSTRACT

Introduction: Lung cancer remains one of the leading causes of cancer-related mortality worldwide. Despite advances in diagnostic imaging, histopathological assessment continues to be the gold standard for accurate classification of lung cancer subtypes. However, manual interpretation of histopathological slides is time-consuming and susceptible to inter-observer variability, underscoring the need for efficient Computer-Aided Diagnostic (CAD) systems.

Aim: To develop a Convolutional Neural Network (CNN)-based model for automated classification of lung carcinoma histopathological images by integrating classical gradient-based edge detection techniques to enhance image quality and improve classification performance.

Materials and Methods: This retrospective analytical study was conducted in the ICMR-funded laboratory at Brainware University, Kolkata, West Bengal, India. The project commenced in February 2024 and is proposed to conclude in February 2027. To date, it has yielded a dataset of 11,580 histopathological images of lung tissue, categorised as Lung Adenocarcinoma (LUAD), Lung Squamous Cell Carcinoma (LSCC), and Non Malignant (BNM). The present work represents a split study and forms part of a larger ICMR-funded project spanning three years. This component focuses on LUAD, LSCC, and non-malignant lung tissue, thereby encompassing the two most common Non Small Cell Lung Cancer (NSCLC) subtypes (which together account for approximately 85% of lung cancers) along with a normal reference class. Edge enhancement was performed using Sobel and Scharr operators to emphasise structural boundaries. The processed images were used to train a custom-designed CNN architecture comprising three convolutional blocks, each followed by pooling layers, and fully connected layers for classification. The model was trained for 100 epochs with a batch size of 32 and evaluated using accuracy, precision, sensitivity, specificity, and F1-score as performance metrics.

Results: Sobel-based preprocessing yielded superior model performance compared with the Scharr method. The proposed CNN trained on Sobel-enhanced images achieved an overall classification accuracy of 93.55%, outperforming the 81.33% accuracy obtained with Scharr-based preprocessing. The Sobel-enhanced model also demonstrated stronger generalisation, with AUC values of 0.98, 1.00, and 0.98 for the LUAD, BNM, and LSCC classes, respectively.

Conclusion: The integration of edge detection with CNN-based analysis effectively enhances the classification of lung cancer histopathological images. The Sobel operator notably improved model accuracy, precision, and generalisation, suggesting its potential suitability for highlighting morphological boundaries in tissue sections. Future work will extend this framework by exploring additional edge detection methods, implementing stain normalisation, and validating performance on external datasets to further optimise model robustness and clinical applicability.

Keywords: Lung carcinoma, Machine learning, Scharr, Sobel

INTRODUCTION

Cancer remains one of the most pressing health concerns of the 21st century, affecting millions of individuals worldwide. Among the various malignancies, lung cancer is the leading cause of cancer-related mortality globally, as reported by the World Health Organisation (WHO) [1]. In 2022, the International Agency for Research on Cancer (IARC) documented approximately 2.43 million newly diagnosed lung cancer cases and nearly 1.77 million deaths, underscoring its devastating global impact. Within India, the burden is equally alarming, with 81,748 new cases and 75,031 deaths attributed to lung cancer in the same year [2]. Furthermore, projections indicate a dramatic rise in the national incidence rate from 0.082 million in 2022 to nearly 0.156 million by 2045- reflecting an increase of about 90.2% [3].

According to the WHO classification, more than 95% of lung cancers are categorised into two key histological types: Non Small Cell Lung Cancer (NSCLC) and Small Cell Lung Carcinoma (SCLC) [4]. NSCLC includes three primary subtypes- adenocarcinoma, squamous cell carcinoma, and large cell carcinoma [5]. Notably, NSCLC accounts for approximately 85% of lung cancer cases, whereas SCLC represents the remaining 15% [6]. Despite substantial advances in therapeutic strategies, the overall prognosis for lung cancer remains poor, largely due to late detection and diagnosis at advanced stages of the disease [7].

Current diagnostic procedures for lung carcinoma primarily rely on imaging modalities such as Computed Tomography (CT), Positron Emission Tomography-Computed Tomography (PET-CT), chest X-rays, and bronchoscopy [8]. However, histopathological

evaluation of biopsy samples continues to serve as the gold standard for definitive diagnosis [9]. These tissue samples are commonly stained with Haematoxylin and Eosin (H&E) to enable microscopic visualisation of cellular and structural features [10]. Manual inspection of H&E-stained slides, however, is labour-intensive, time-consuming, and prone to human error [11]. Inter-observer variability among pathologists further contributes to diagnostic inconsistencies, underscoring the need for computer-assisted solutions [12].

The advent of digital pathology and CAD systems has revolutionised cancer diagnosis by enabling objective and reproducible evaluations [13]. In particular, deep learning-based CNNs have exhibited exceptional performance across a range of medical image analysis tasks, including cancer detection and classification [14,15]. Additionally, edge detection methods play a pivotal role in enhancing the quality of histopathological images, thereby improving diagnostic precision and supporting treatment planning.

In the present study, the authors propose a deep learning framework for classifying lung carcinoma using histopathological images. The approach incorporates classical gradient-based edge detection techniques for image enhancement prior to classification. The developed model is rigorously evaluated using multiple performance metrics to assess its diagnostic accuracy and reliability.

MATERIALS AND METHODS

This retrospective analytical study was conducted in the ICMR-funded laboratory at Brainware University, Kolkata, West Bengal, India. The project commenced in February 2024 and is proposed to conclude in February 2027. They utilised a previously curated histopathological image dataset generated under an ongoing ICMR-funded project for lung carcinoma classification. The study was conducted in the ICMR-funded Laboratory of Brainware University in collaboration with Gujarat Cancer Research Institute and Apollo, Kolkata, West Bengal, India. The study was started in February 2024. The study is 3 of years and is proposed to be completed by February 2027. Ethical approval was obtained from the Institutional Ethics Committee of Brainware University (Approval No. EC-BHR-0-14-2024; Approval Date: 19/11/2024). This split study investigates the impact of two edge detection (Sobel and Scharr) techniques on the performance of deep learning models for lung cancer classification as part of a broader project aimed at developing robust deep learning–based diagnostic systems.

Inclusion criteria:

- Whole Slide Images (WSIs) containing clearly identifiable Regions Of Interest (ROIs) annotated by expert medical consultants;
- Image tiles belonging to the three predefined classes: LUAD, LSCC, and Non malignant lung tissue (BNM).

Exclusion criteria:

- Histopathological images that were blurred, poorly stained, or contained significant artifacts that could affect model training;
- Duplicate images or patches that did not meet the standardised resolution and preprocessing requirements.

Study Procedure

In the proposed study, a dataset consisting of 11,580 images is used for the development of the ML model [Table/Fig-1]. The dataset is divided into three classes: LUAD, LSCC and Non Malignant (BNM). The histopathological images used in this study were extracted from 300 WSIs of the cancerous tissues of the Lung, where the ROI were manually annotated by three medical consultants. The WSIs used for preparing the dataset were retrieved and downloaded from The Cancer Imaging Archive (TCIA). Each image present in the dataset was extracted with a resolution of 512×512 pixels.

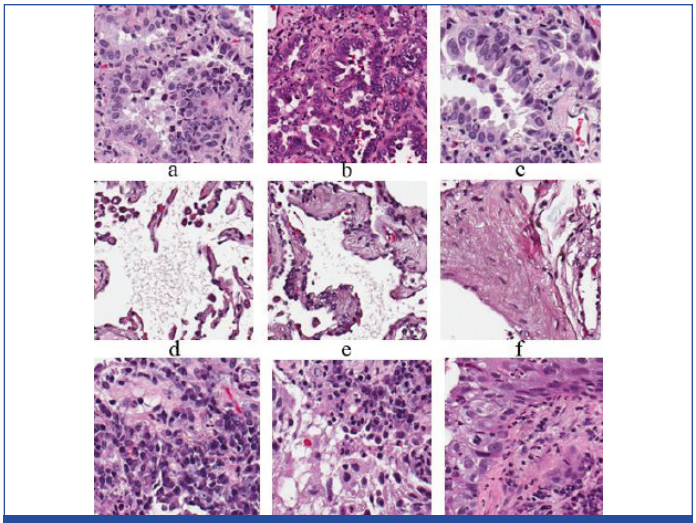

[Table/Fig-1]: Lung carcinoma dataset: a-c) LUAD; d-f) BNM; g-h) LSCC. The images were exported at 10x magnification. All slides were stained with H&E stain.

Image Pre-processing: Image Pre-processing is a fundamental step in any Machine Learning (ML) methodology. Resizing and rescaling are carried out to introduce uniformity in the dataset and for faster convergence during model training. In this proposed work, edge detection is carried out to improve the overall clarity of the image features and reduce noise present in the images [16]. Gradient-based operators such as Sobel and Scharr edge detection methods are used in the dataset.

a) Sobel edge detection: The Sobel operator is a popular edge detection method that leverages gradient information. Applying 3×3 convolutional kernels along both horizontal and vertical directions offers improved precision over earlier techniques such as the Robert operator, particularly in detecting diagonal edges [17].

b) Scharr edge detection: This edge detection method improves gradient estimation by employing specially tuned filters that enhance rotational symmetry. Unlike traditional techniques such as the Sobel operator, the Scharr operator offers greater accuracy in identifying edges, particularly those with diagonal or curved orientations [18].

Proposed CNN architecture: The deep learning model for lung cancer classification utilised a CNN-based architecture, as displayed in [Table/Fig-2]. It is mainly divided into two parts. Primarily, the features are extracted, and then the features are flattened and passed on to the classification network for lung cancer classification. The architecture follows this pattern: {{(2 Conv × 1 MaxPool) * 3} + 1 Flatten + 3 FC + 1 output}. The convolutional layers used 3×3 filters to perform element-by-element matrix multiplication on the input images, enabling the network to extract spatial features. To reduce the computational load and reduce feature map dimensions, pooling layers were incorporated after the convolutions. The three successive convolutional blocks contained 16, 32, and 64 filters, respectively, progressively increasing the model's capacity to learn complex features. After feature extraction, the output was flattened and passed through three fully connected layers, which established weighted connections between neurons to support the classification task. These layers applied standard computations to transform the features into a suitable format for the final prediction. A SoftMax function was then applied at the output layer to generate a probability distribution over the possible classes.

Experimental setup: The whole experiment was conducted in a DELL workstation equipped with an Intel Xeon W5 16-core 2.0GHz to 4.2GHz (Turbo 220W) processor, 128GB of RAM, and an NVIDIA A6000 GPU (48 GB) Video RAM for model training. Visual Studio Code was used as an IDE and experiments were carried out using various machine learning libraries such as TensorFlow, Keras, scikit-learn, etc in Python.

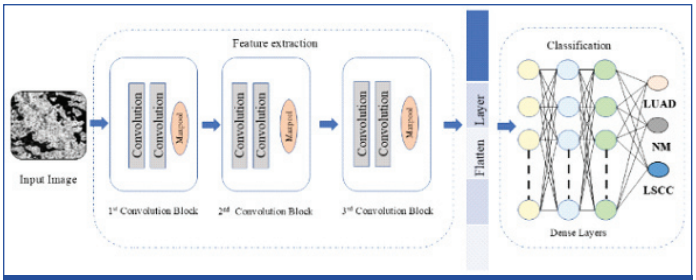

[Table/Fig-2]: Proposed CNN architecture.

Performance evaluation of the proposed model: The proposed lung cancer classification model is trained with 80% of images from the lung carcinoma dataset. The rest 20% is used for model validation and testing. The ML model was trained for 100 epochs with a batch size of 32. Primarily, for the assessment of the quality of edge detection, a set of metrics such as precision, recall, and dice scores was calculated. Performance evaluation of the model was carried out using different assessment metrics such as accuracy, sensitivity, specificity, and F1-Score, depicted in equations 1-5.

$$\text{Accuracy} = \frac{T^{+}+T^{'}}{T^{+}+T^{'}+F^{+}+F^{'}} \quad (1)$$

$$\text{Precision} = \frac{T^{+}}{T^{+}+F^{+}} \quad (2)$$

$$\text{Sensitivity} = \frac{T^{+}}{T^{+}+F^{'}} \quad (3)$$

$$\text{Specificity} = \frac{T^{'}}{T^{'}+F^{+}} \quad (4)$$

$$\text{F1-Score} = \frac{2T^{+}}{2T^{+}+F^{'}+F^{+}} \quad (5)$$

Where T^{+} represents True Positive, $T^{'}$ is True Negative, F^{+} s False Positive and $F^{'}$ is False Negative.

STATISTICAL ANALYSIS

No explicit statistical software was used in this study. Standard Machine learning based metrics for Deep learning model assessment and image quality assessment metrics was used in this study.

RESULTS

Assessment of Edge Detection of Lung Carcinoma Images

Sobel and Scharr operators exhibit distinct characteristics across the three classes of lung tissue As observed in [Table/Fig-3a-c]. In LUAD [Table/Fig-3a], Sobel effectively captured both subtle and coarse edges, preserving fine structural details, whereas Scharr produced clearer and more continuous glandular and epithelial boundaries. In BNM [Table/Fig-3b], Sobel highlighted numerous small-intensity edges that may correspond to diagnostically relevant fine tissue features, while Scharr more effectively suppressed noisy boundaries and focused on prominent structural outlines. Furthermore, in LSCC [Table/Fig-3c], Sobel delineated edges within dense and overlapping cell areas, providing comprehensive boundary information, whereas Scharr highlighted selected important boundaries more distinctly.

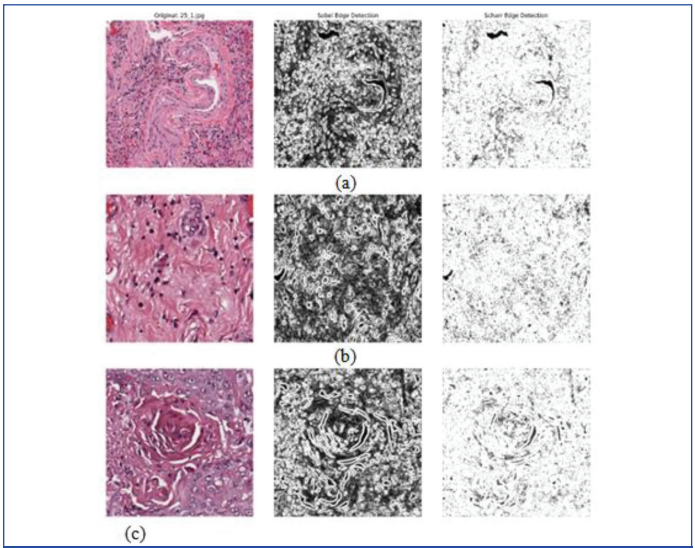

[Table/Fig-3]: Edge detected image (Sobel and Scharr): a) LUAD; b) BNM; c) LSCC.

Although qualitative visual inspection suggests that Scharr yields cleaner and more selective edges for certain classes, the quantitative evaluation presented in [Table/Fig-4] shows that Sobel achieves a superior balance of precision and recall. This results in marginally higher Dice scores for BNM (0.61 vs. 0.59) and LSCC (0.57 vs. 0.56), with equal performance in LUAD. This more balanced edge representation translates into improved generalisation and higher classification accuracy when the images are used as input to the downstream CNN model.

Class	Edge detection method	Precision	Recall	Dice score
LUAD	Sobel	0.62	0.92	0.72
	Scharr	0.60	0.99	0.72
BNM	Sobel	0.49	0.92	0.61
	Scharr	0.45	0.96	0.59
LSCC	Sobel	0.44	0.94	0.57
	Scharr	0.44	0.96	0.56

[Table/Fig-4]: Comparative assessment of edge detection methods on the dataset.

A comparative evaluation of the Sobel and Scharr edge detection methods for three histopathological classes—LUAD, BNM, and LSCC—is presented in [Table/Fig-4]. The Scharr operator consistently achieves higher recall across all classes (0.99 for LUAD and 0.96 for both BNM and LSCC), indicating greater sensitivity in detecting prominent tissue boundaries. In contrast, Sobel demonstrates slightly higher precision, particularly in LUAD (0.62 vs. 0.60), suggesting fewer false-positive detections. With respect to the Dice score, both methods achieve identical performance in LUAD (0.72), while Sobel marginally outperforms Scharr in BNM (0.61 vs. 0.59) and LSCC (0.57 vs. 0.56). Overall, although Scharr exhibits superior recall, Sobel provides a slightly better balance between precision and recall, leading to comparable or marginally improved segmentation performance across the evaluated classes.

Training and Validation Curves of the Proposed Model

the convergence curves of the proposed model trained on the edge-enhanced dataset are plotted in [Table/Fig-5a,b]. It helps in observing model performance during the training phase- whether it is suffering from overfitting or underfitting.

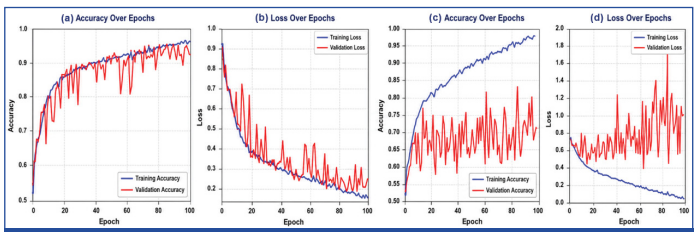

[Table/Fig-5]: Training and validation accuracy and Loss of the Model on Edge Detected dataset (a) Sobel; (b) Scharr.

The model trained with the Sobel operator shows robust and consistent performance, with training and validation accuracy increasing together, subject to only moderate fluctuations. The loss curves also decline steadily, indicating stable convergence and good generalisation. In contrast, the model trained with the Scharr operator exhibits overfitting. Although the training accuracy is high, the validation accuracy is unstable and does not increase consistently across epochs. The training loss decreases, but the

validation loss fluctuates and does not decrease in tandem with the training loss.

In summary, the Sobel-based model demonstrates better generalisation and stability across training and validation, while the Scharr-based model suffers from significant overfitting despite achieving high training performance.

The confusion matrices for the developed model trained on the processed dataset are depicted in [Table/Fig-6]. Here, the numbers of TP, TN, FP, and FN are calculated, which are essential for determining various assessment metrics for model performance.

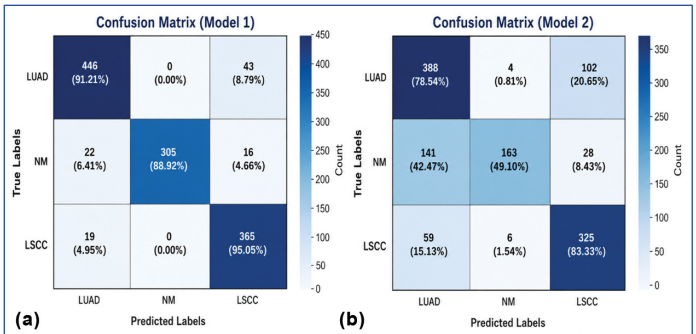

[Table/Fig-6]: Confusion Matrix of the model on edge detected dataset: a) Sobel; b) Scharr.

Performance evaluation of the model is carried out, across various classes for Sobel and Scharr processed dataset in [Table/Fig-7]. The various performance metrics such as accuracy, precision, specificity, etc., are calculated based on the number of TP, TN, FP and FN, derived from confusion matrices, displayed in [Table/Fig-4]. With Sobel, the model achieved superior performance across all classes. LUAD achieved an accuracy of 0.93 and 0.91 F1-score, BNM recorded 0.97 accuracy, 1.00 precision, and 0.94 F1-score, while LSCC reached 0.94 accuracy and 0.90 F1-score. These values reflect high precision, sensitivity, and specificity, indicating strong and balanced classification.

Model	Edge detection	Class	Assessment metrics				
			ACC	PRE	SEN	SPE	F1-SCORE
Proposed model	Sobel	LUAD	0.93	0.92	0.91	0.94	0.91
		BNM	0.97	1.00	0.89	1.00	0.94
		LSCC	0.94	0.86	0.95	0.93	0.90
	Scharr	LUAD	0.75	0.66	0.79	0.72	0.72
		BNM	0.85	0.94	0.49	0.99	0.65
		LSCC	0.84	0.71	0.83	0.84	0.77

[Table/Fig-7]: Performance comparison of the model on edge detected dataset.

In contrast, the model trained with the Scharr dataset led to reduced performance. LUAD had 0.75 accuracy and 0.72 F1-score, and BNM showed 0.85 accuracy but low sensitivity (0.49) despite high precision (0.94), resulting in an F1-score of 0.65. LSCC performed better than LUAD and BNM under Scharr, with 0.84 accuracy and 0.77 F1-score. In summary, the Sobel operator obtained consistently better performance compared to Scharr, making it a more effective edge detection method for this classification model.

Classification: ROC Curve and AUC

The ROC curves aid in assessing the class-wise performance of the model, trained on different edge-enhanced datasets [Table/Fig-8a,b]. The model trained on the Sobel-filtered dataset achieves excellent classification among the different classes, with high AUC values for all classes (LUAD: 0.98, BNM: 1.00, LSCC: 0.98), indicating strong and confident classification. In contrast, the model trained on the Scharr enhanced dataset performs less effectively, with lower AUC scores (LUAD: 0.86, BNM: 0.89, LSCC: 0.89), depicting weaker classification performance and increased overlap between classes.

DISCUSSION

The present study demonstrated integrating classical gradient-based edge detection with a custom-designed CNN for precise classification of histopathological images of lung carcinoma. In contrast to several recent studies that primarily rely on large pre-trained architectures and ensemble strategies, such as Vijh S et al., (97.18% accuracy on 120 CT images) and Gowthamy J and Ramesh S (98.9% accuracy using ResNet-50, InceptionV3, and DenseNet on LC25000), the proposed method emphasises structured image enhancement combined with a relatively lightweight CNN trained from scratch [19,20]. Despite its architectural simplicity, the proposed model achieved high class-wise accuracies of 0.93 (LUAD), 0.97 (BNM), and 0.94 (LSCC) using Sobel-enhanced images, demonstrating the effectiveness of targeted preprocessing in histopathological analysis.

On evaluating the two edge detection methods, Scharr achieved higher recall values (0.99 for LUAD and 0.96 for BNM and LSCC), indicating greater edge sensitivity. However, this increased sensitivity was accompanied by lower precision values (0.60 for LUAD, 0.45 for BNM, and 0.44 for LSCC) and slightly lower Dice scores in BNM (0.59) and LSCC (0.56), while remaining equal in LUAD (0.72). This imbalance in precision–recall trade-off translated into reduced classification performance after CNN training. Specifically, Scharr-based preprocessing resulted in class-wise accuracies of 0.75 (LUAD), 0.85 (BNM), and 0.84 (LSCC), with F1-scores ranging from 0.65 to 0.77. Notably, the sensitivity for BNM dropped to 0.49 despite high precision (0.94), indicating unstable generalisation and potential overfitting behavior. Similar issues of excessive edge sensitivity and noise amplification have been reported in comparative edge detection analyses by Mayangsari AD and Agung IWP [21].

In contrast, Sobel-based pre-processing produced more balanced edge representations, which improved downstream classification stability. The Sobel-enhanced CNN achieved class-wise accuracies of 0.93 (LUAD), 0.97 (BNM), and 0.94 (LSCC), with corresponding F1-scores of 0.91, 0.94, and 0.90, respectively. Sensitivity values remained consistently high (0.91 for LUAD, 0.89 for BNM, and 0.95 for LSCC), reflecting better class-wise generalisation. ROC analysis further demonstrated strong discriminative capability, with AUC values of 0.98 for LUAD, 1.00 for BNM, and 0.98 for LSCC. These results suggest that Sobel filtering effectively emphasises diagnostically relevant morphological boundaries- such as glandular formations in adenocarcinoma and keratinised structures in squamous cell carcinoma- while suppressing irrelevant high-frequency noise. This observation aligns with morphology-centric findings reported by Faria N et al. and Ignatov A et al., who emphasised the importance of structural cues in histopathological classification [22,23].

When benchmarked against recent state-of-the-art transfer learning approaches, the proposed model demonstrates competitive performance despite using fewer parameters and no pre-trained weights. For example, Ochoa-Ornelas R et al., reported 99.39% accuracy using EfficientNetB3 on 25,000 images, and Savaş and Güler achieved 99.78% accuracy using a seven-model ensemble [24,25]. Although these approaches yield higher numerical accuracy, they rely on substantial computational resources and complex ensemble frameworks. In contrast, the proposed Sobel-CNN framework demonstrates competitive performance on internal validation with significantly reduced architectural complexity, which may offer practical advantages in settings with limited computational resources.

Compared to multimodal and prognosis-oriented frameworks, such as the multimodal fusion network by Sangeetha SKB et al., (92.5% accuracy) or the recurrence prediction model by Kim PJ et al., (AUC = 0.763), the present study focuses specifically on histopathological subtype classification [25,26]. The AUC values approaching unity indicate that even unimodal histopathology-based systems can achieve highly reliable diagnostic performance when appropriate preprocessing strategies are applied.

Limitation(s)

In the proposed study, only two classical edge detection techniques were employed, without evaluating other edge detection operators or stain normalisation methods, which may reduce robustness to the staining variability present in the dataset. Moreover, although the dataset was derived from 300 WSIs from TCIA, external multicentre validation was not performed, potentially limiting the generalisability of the findings. Finally, the study included only LUAD, LSCC, and non malignant tissue, excluding SCLC and rare subtypes. The CNN was trained from scratch without incorporating transfer learning or explainability methods, and prospective clinical validation was not undertaken. Future studies will focus on addressing these limitations.

CONCLUSION(S)

Lung cancer remains a major global health burden with a very high mortality rate. In this study, we investigated the effects of gradient-based edge detection methods within a deep learning model. Among the approaches evaluated, the Sobel operator outperformed the Scharr operator, demonstrating superior performance on the present dataset as evidenced by both statistical metrics and ROC analysis. The model trained on the Sobel-processed dataset achieved an accuracy of 93.55%, surpassing the Scharr-based approach, which reached 81.33%. However, this study was limited to Sobel and Scharr edge detection and did not include colour normalisation, external dataset validation, or interpretability analyses. Future work will incorporate additional edge detection techniques and stain normalisation to improve image preprocessing and will validate performance on external datasets.

Acknowledgement

The authors gratefully acknowledge the Indian Council of Medical Research (ICMR) for providing the essential funding that made this research possible. The authors also wish to acknowledge the Centre for Multidisciplinary Research and Innovation (CMRI), and the Department of Computational Sciences at Brainware University, Barasat, West Bengal, for their crucial infrastructure support.

Funding: This study was supported by a grant from the Indian Council of Medical Research (ICMR), number EM/SG/Dev. Res/120/0847-2023 dated 08/02/2024.

REFERENCES

[1] International Agency for Research on Cancer. Cancer TODAY [Internet]. Lyon: IARC; 2022. [cited 2025 Oct 7]. Available from: https://gco.iarc.who.int.
[2] Indian Council of Medical Research–National Centre for Disease Informatics and Research. Decade of research: Impacting NCD public health actions 2022 [Internet]. Bengaluru: ICMR–NCDIR; 2022. [cited 2025 Oct 7]. Available from: https://www.ncdirindia.org/All_Reports/Monograph2022/ICMR_NCDIR_Monograph.pdf.
[3] International Agency for Research on Cancer. Cancer tomorrow: Estimated number of new cases from 2022 to 2045, trachea, bronchus and lung, India [Internet]. Lyon: IARC; 2023. [cited 2025 Oct 7]. Available from: https://gco.iarc.fr/tomorrow/en/dataviz/bubbles?populations=356&cancers=15.
[4] Travis WD, Brambilla E, Noguchi M, Nicholson AG, Geisinger KR, Yatabe Y, et al. International Association for the Study of Lung Cancer/American Thoracic Society/European Respiratory Society international multidisciplinary classification of lung adenocarcinoma. J Thorac Oncol. 2011;6(2):244-85.
[5] Ricotti A, Sciannameo V, Balzi W, Roncadori A, Canavese P, Avitabile A, et al. Incidence and prevalence analysis of non-small-cell and small-cell lung cancer using administrative data. Int J Environ Res Public Health. 2021;18(17):9076.
[6] Basumallik N, Agarwal M. Cancer, lung small cell (oat cell) [Internet]. Treasure Island (FL): StatPearls Publishing; 2019 [cited 2025 Oct 7]. Available from: https://www.ncbi.nlm.nih.gov/books/NBK482458,
[7] Xu Y, Hosny A, Zeleznik R, Parmar C, Coroller T, Franco I, et al. Deep learning predicts lung cancer treatment response from serial medical imaging. Clin Cancer Res. 2019;25(11):3266-75.
[8] Tippannavar S, Yashwanth SD, Shivakumar G, Madappa E. Revolutionizing lung cancer diagnosis: A comprehensive review of image processing techniques for early detection and precision medicine. J Innov Image Process. 2023;5:337-57.
[9] Nooreldeen R, Bach H. Current and future development in lung cancer diagnosis. Int J Mol Sci. 2021;22(16):8661.
[10] Fischer AH, Jacobson KA, Rose J, Zeller R. Hematoxylin and eosin staining of tissue and cell sections. CSH Protoc. 2008;2008(6):pdb.prot4986.
[11] Sinha S, Mali S, Rajkhowa S. High-precision lung cancer classification with custom CNN: Evaluation and transfer learning for broader cancer types. Procedia Comput Sci. 2025;258:3922-33.
[12] Elmore JG, Longton GM, Carney PA, Geller BM, Onega T, Tosteson AN, et al. Diagnostic concordance among pathologists interpreting breast biopsy specimens. JAMA. 2015;313(11):1122-32.
[13] Noaman NF, Kanber BM, Al Smadi A, Jiao L, Alsmadi MK. Advancing oncology diagnostics: AI-enabled early detection of lung cancer through hybrid histological image analysis. IEEE Access. 2024;12:64396-415.
[14] He K, Zhang X, Ren S, Sun J. Delving deep into rectifiers: Surpassing human-level performance on ImageNet classification. In: Proc IEEE Int Conf Comput Vis. 2015. p. 1026-34.
[15] Esteva A, Kuprel B, Novoa RA, Ko J, Swetter SM, Blau HM, et al. Dermatologist-level classification of skin cancer with deep neural networks. Nature. 2017;542(7639):115-18.
[16] Savaş S, Güler O. Ensemble learning based lung and colon cancer classification with pre-trained deep neural networks. Health Technol. 2025;15(1):105-17.
[17] Sobel I, Feldman G. A 3×3 isotropic gradient operator for image processing. In: Duda R, Hart P, editors. Pattern classification and scene analysis. New York: Wiley; 1973. p. 271-72.
[18] Scharr H. Optimal operators in digital image processing [dissertation]. Heidelberg: University of Heidelberg; 2000.
[19] Vijh S, Gaurav P, Pandey HM. Hybrid bio-inspired algorithm and convolutional neural network for automatic lung tumor detection. Neural Comput Appl. 2023;35:23711-24.
[20] Gowthamy J, Ramesh S. A novel hybrid model for lung and colon cancer detection using pre-trained deep learning and KELM. Expert Syst Appl. 2024;252:124114.
[21] Mayangsari AD, Agung IWP. A systematic literature review: Performance comparison of edge detection operators in medical images. J ELTIKOM. 2024;8(1):09-25.
[22] Faria N, Campelos S, Carvalho V. A novel convolutional neural network algorithm for histopathological lung cancer detection. Appl Sci. 2023;13(11):6571.
[23] Ignatov A, Yates J, Boeva V. Histopathological image classification with cell morphology aware deep neural networks. In: Proc IEEE/CVF Conf Comput Vis Pattern Recognit Workshops. 2024.
[24] Ochoa-Ornelas R, Gudiño-Ochoa A, García-Rodríguez JA, Uribe-Toscano S. A robust transfer learning approach with histopathological images for lung and colon cancer detection using EfficientNetB3. Healthc Anal. 2025;7:100391.
[25] Sangeetha SKB, Mathivanan SK, Karthikeyan P, Rajadurai H, Shivahare BD, Mallik S, et al. An enhanced multimodal fusion deep learning neural network for lung cancer classification. Syst Soft Comput. 2024;6:200068.
[26] Kim PJ, Hwang HS, Choi G, Sung HJ, Ahn B, Uh JS, et al. A new model using deep learning to predict recurrence after surgical resection of lung adenocarcinoma. Sci Rep. 2024;14:6366.

PARTICULARS OF CONTRIBUTORS:
1. Project Technical Support-III, Department of Department of Computational Sciences, Brainware University, Barasat, West Bengal, India.
2. Project Intern, Department of Computational Sciences, Brainware University, Barasat, West Bengal, India.
3. Associate Professor, Department of Oncopathology, The Gujarat Cancer and Research Institute, Ahmedabad, Gujarat, India.
4. Senior Consultant, Department of Oncopathology (Histopathology), Apollo Hospital, Kolkata, West Bengal, India.
5. Resident, Department of Oncopathology, The Gujarat Cancer and Research Institute, Ahmedabad, Gujarat, India.
6. Assistant Professor, Center for Biotechnology and Bioinformatics, Dibrugarh University, Dibrugarh, Assam, India.
7. Professor, Department of Computational Sciences, Brainware University, Kolkata, West Bengal, India.

NAME, ADDRESS, E-MAIL ID OF THE CORRESPONDING AUTHOR:
Dr. Subrata Sinha,
Professor, Department of Computational Sciences, Brainware University,
Barasat-700125, West Bengal, India.
E-mail: subratasinha2020@gmail.com

PLAGIARISM CHECKING METHODS: [Jain H et al.]
- Plagiarism X-checker: Nov 06, 2025
- Manual Googling: May 12, 2026
- iThenticate Software: May 14, 2026 (6%)

ETYMOLOGY: Author Origin

EMENDATIONS: 8

AUTHOR DECLARATION:
- Financial or Other Competing Interests: As declare above
- Was Ethics Committee Approval obtained for this study? Yes
- Was informed consent obtained from the subjects involved in the study? Yes
- For any images presented appropriate consent has been obtained from the subjects. Yes

Date of Submission: **Oct 22, 2025**
Date of Peer Review: **Jan 02, 2026**
Date of Acceptance: **May 16, 2026**
Date of Publishing: **Aug 01, 2026**